# Effects of Nonlinearities on Ground Resonance Instability

Giulio Avanzini*
Politecnico di Torino, Turin, 10129, Italy
and
Guido de Matteis†
"Sapienza" Università di Roma, Rome, 00184, Italy

## Abstract

This paper presents a bifurcation analysis of the ground resonance phenomenon in order to investigate the effects of nonlinearities in the instability experienced by a simplified helicopter model. Using a numerical continuation method, the stability boundaries of the system and the characteristics of the periodic motion are determined, to demonstrate the advantages and potential of the methodology when dealing with critical situations featuring a sudden loss of stability as well as in those situations where a quantitative determination of post–critical behavior is of relevant interest.

### Nomenclature

$e$ blade lag hinge eccentricity
$I$ blade moment of inertia around hinge axis
$m$ $= m_0 + nm$, total vehicle mass
$m_b$ blade mass
$m_0$ fuselage mass
$n$ number of blades
$n_b$ blade lag damping coefficient
$n_0$ fuselage damping coefficient
$p_0$ fuselage undamped natural frequency
$s$ Laplace variable
$S$ blade static moment w.r.t. lag hinge
$t$ time
$x$ fuselage lateral displacement
$\boldsymbol{y}$ $= (x, \eta, \phi)^T$, system state vector

Greek symbols
$\delta^2$ fuselage cubic stiffening term coefficient
$\gamma$ fuselage nonlinear damping coefficient
$\epsilon$ $= nS^2/(2mI)$, hinged mass inertial parameter
$\eta$ rotor c.g. lateral displacement parameter
$\nu_0$ $= (eS/I)^{0.5}$, blade inertial parameter
$\xi_k$ $k$–th blade lag angle
$\tau$ nondimensional time
$\phi$ rotor c.g. longitudinal displacement parameter
$\psi_k$ $k$–th blade anomaly
$\omega$ rotor angular speed

Subscripts and superscripts
$\dot{(\,)}$ differentiation with respect to time $t$
$(\,)'$ differentiation with respect to nondimensional time $\tau$
$\tilde{(\,)}$ generalized (state variable or parameter)

## 1 Introduction

In this paper an analysis approach based on the use of numerical continuation methods [1, 2] and bifurcation analysis [3] is proposed as a means for investigating the ground resonance phenomenon and, in particular, the effects of nonlinearities on the post–critical behaviour, once the loss of stability of the equilibrium condition triggers wide amplitude oscillations of the rotor–fuselage–undercarriage system.

The well known ground resonance instability develops as a result of the interaction between rotor blade lag motion and elasticity of the undercarriage, and may cause serious damage to the helicopter, up to catastrophic break–down of rotor or structure, during either the landing or take-off phases. The principal objective of the study is to devise and demonstrate a design tool which highlights possible critical features of a specified rotorcraft configuration when certain system parameters are varied. Accordingly, the stability boundaries and the features of the periodic motion are characterized for a simplified helicopter model [4], which retains all the features necessary for describing the ground resonance phenomenon.

*Assistant Professor, Department of Aerospace Engineering, C.so Duca degli Abruzzi 24, e–mail: *giulio.avanzini@polito.it*, tel. +39 011 5646831, fax +39 011 5646899; AIAA Senior Member.

†Professor, Department of Mechanics and Aeronautics, Via Eudossiana 18, e–mail: *dematteis@dma.ing.uniroma1.it*, tel. +39 06 44585210, fax +39 06 4882576; AIAA Senior Member.

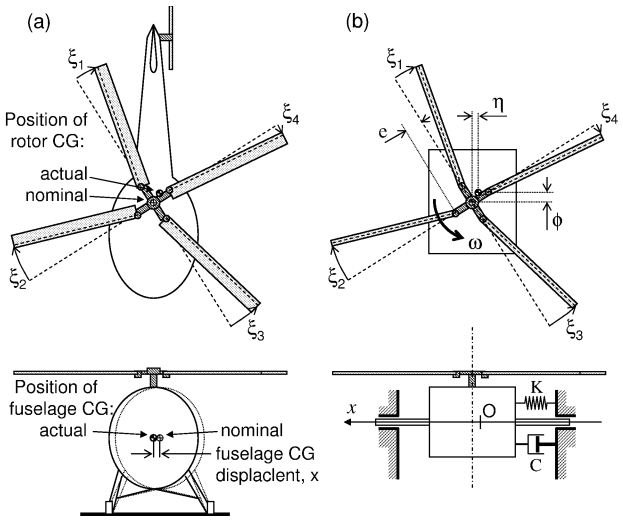


Figure 1: Origin of the ground resonance phenomenon (a) and simplified model (b).

Several studies were devoted in the past to analyze this problem and determine stability boundaries for blade and undercarriage parameters. Coleman and Feingold [5] first provided the correct physical interpretation of ground resonance as a self–excited mechanical oscillation, related to a coupling between rotor centre of mass displacement with respect to the shaft axis, induced by different values of the lag angle for the rotor blades, and the elasticity of the undercarriage. Aerodynamic forces play little role (if any) in the loss of stability of the coupled rotor–fuselage system. Based on these findings, Mil and his co–workers [4] derived a simple mathematical model for the analysis of fuselage and blade lag motion, which features only those characteristics crucial for the onset of ground resonance oscillations. In particular, $n$ rotor blades are connected through lead-lag hinges to a hub rotating at an angular speed $\omega$, and the rotor shaft is mounted on a fuselage of mass $m_0$, with a lateral translational degree of freedom which is representative of lateral motion of the helicopter on its landing gear. Elasticity and damping of the undercarriage are described by means of a spring and a damper, respectively (Fig. 1). No displacements in either the longitudinal and vertical directions are considered in the model, nor aerodynamic forces on the rotor blades.

When linear stiffness and damping terms are considered, motion of the helicopter is described by a system of $n+1$ second order, linear ordinary differential equations with periodic coefficients. A reduced order system represented by a set of 3 second–order linear ordinary differential equations with constant coefficients can be derived for stability analysis, where individual blade motion is not dealt with and the only states are fuselage lateral displacement and longitudinal and lateral rotor c.g. coordinates, that depend on blade lag angles and anomaly. Starting from this model, Mil *et al.* [4] provide conditions for the onset of ground resonance oscillations for the small perturbation linear case. The study was later extended by Tongue [6], dealing with the effects of nonlinearities in the damping term of the undercarriage on the onset of limit cycle behaviour when the stability threshold is crossed. The analysis was carried out by means of an approximation of the nonlinear term based on the describing function approach [7], also known as "quasi–linearization". Post–critical behaviour was determined by tracing plots of limit cycle amplitude as a function of system parameters.

In this paper, the numerical continuation method is used to trace branches of periodic solutions [2] so as to perform a similar study for the original nonlinear model, that is, without approximating the effects of nonlinear terms by the describing function. As a major advantage, this approach can deal with more complex scenarios, *e.g.* where nonlinearities in the stiffness term of the undercarriage model are also included. As an example, a cubic stiffening term in the undercarriage response is introduced that can be hardly approximated by quasi–linearization.

The capabilities of bifurcation analysis [3] and continuation methods [1, 2] to efficiently assess stability properties as a function of system parameters has been widely exploited in the past in order to investigate critical flight regimes of fixed wing aircraft in the presence of nonlinear phenomena (see [8] and references therein). In spite of the considerable success of this approach in investigating instabilities related to variations of flight condition or design parameters, the methodology has been seldom considered for analyzing critical behavior for rotary–wing aircraft. To the best of the authors' knowledge, the first application of catastrophe theory to a problem related with helicopter rotor instabilities is due to Afolabi [9], but only more recently continuation methods were employed for detecting bifurcations along equilibrium branches of rotor models in a way similar to that proposed for fixed wing aircraft. This was done in [10] on a relatively simple model, featuring an averaged description of rotor force and moments. Instabilities and jump phenomena determined by means of bifurcation theory were then verified by direct sim-

ulation for a more complex, individual blade rotor model.

Investigation of the ground resonance phenomenon allows for outlining the main features of the proposed approach, while demonstrating its potential for investigating critical situations where sudden loss of stability are expected, together with a quantitative description of the expected post–critical behaviour. After tracing bifurcation diagrams by means of the continuation method, ground resonance instability is investigated in the framework of catastrophe theory, as proposed in [6] and [9], for a wider set of model nonlinearities.

The model used for the analysis [4, 6] is briefly recalled in the next section. Some details on the application of continuation methods to the considered system are also given. Nonlinear terms are included in the model and a comparison between the findings obtained from the proposed approach with the simple analytical derivations discussed in [6] is presented in the Section of Results. A paragraph of Conclusions ends the paper.

# 2 Analysis

## 2.1 Rotorcraft Model

A simple yet effective model for the study of ground resonance was derived from first principles by Mil *et al.* [4]. Taking into account Fig. 1 and the Nomenclature section, the equations of the coupled blade–lag and fuselage motion is given by

$$\ddot{x} + (2n_0 + \gamma|\dot{x}|)\dot{x} + p_0^2 x = \tag{1}$$
$$= \frac{S}{M}\sum_{k=1}^{n}\left[(\ddot{\xi}_k - \omega^2\xi_k)\mathrm{Sin}\psi_k + 2\omega\dot{\xi}_k\mathrm{Cos}\psi_K\right]$$

$$\ddot{\xi}_k + 2n_b\dot{\xi}_k + \omega_b^2\xi_k = \tag{2}$$
$$= \frac{S}{I}\ddot{x}\mathrm{Sin}\psi_k \ , \quad k = 1, 2, ..., n$$

where $\omega_b^2 = \nu_0^2\omega^2$ is the centrifugal restoring moment, no hinge spring torque being assumed throughout the paper, while for $\gamma \neq 0$ a nonlinearity is introduced in the damping term [6].

It is possible to analyze system stability for a reduced order model upon definition of two auxiliary variables

$$\eta = \sum_{k=1}^{n}\xi_k\mathrm{Sin}(\psi_k) \ ; \quad \phi = \sum_{k=1}^{n}\xi_k\mathrm{Cos}(\psi_k) \tag{3}$$

where $\eta$ and $\phi$ are proportional to rotor centre of mass shift in the lateral and longitudinal direction, respectively. By summing up Eqs. (2) for $k = 1, 2, ..., n$, multiplied by $\mathrm{Cos}(\psi_k)$ first, and then repeating the sum operation for the same equations multiplied by $\mathrm{Sin}(\psi_k)$, it is possible to replace Eqs. (1) and (2) with the reduced order system

$$\ddot{x} + (2n_0 + \gamma|\dot{x}|)\dot{x} + p_0^2 x = (S/M)\ddot{\eta} \tag{4}$$
$$\ddot{\eta} + 2n_b\dot{\eta} + \omega_s^2\eta - 2\omega(\dot{\phi} + n_b\phi) = \tag{5}$$
$$= (n/2)(S/I)\ddot{x}$$
$$\ddot{\phi} + 2n_b\dot{\phi} + \omega_s^2\phi + 2\omega(\dot{\eta} + n_b\eta) = 0 \tag{6}$$

where $\omega_s^2 = \omega^2(\nu_0^2 - 1)$. Note that for most modern helicopters, $\nu_0^2 \approx 0.1$, so that $\omega_s^2$ is expected to be negative.

The set given by Eqs. (4)–(5) can be written in term of generalized variables, $\tilde{x} = x\gamma$, $\tilde{\eta} = \eta\gamma(S/M)$, and $\tilde{\phi} = \phi\gamma(S/M)$,

$$\tilde{x}'' + (2\tilde{n}_0 + |\tilde{x}'|)\tilde{x}' + \tilde{x} = \tilde{\eta}'' \tag{7}$$
$$\tilde{\eta}'' + 2\tilde{n}_b\tilde{\eta}' + \tilde{\omega}_s^2\eta - 2\tilde{\omega}(\tilde{\phi}' + \tilde{n}_b\tilde{\phi}) = \epsilon\tilde{x}'' \tag{8}$$
$$\tilde{\phi}'' + 2\tilde{n}_b\tilde{\phi}' + \tilde{\omega}_s^2\phi + 2\tilde{\omega}(\tilde{\eta}' + \tilde{n}_b\tilde{\eta}) = 0 \tag{9}$$

where the prime symbol $(\cdot)'$ indicates differentiation with respect to the nondimensional time $\tau = p_0 t$, while all the system parameters are divided by $p_0$, that is, $\tilde{(\cdot)} = (\cdot)/p_0$ (see [6] for more details on the derivation). The nondimensional coefficient $\epsilon = nS^2/(2IM)$ depends on the inertial properties of the system (blade number, moment of inertia and static moment, and fuselage mass). Note that the same set [Eqs. (7)–(9)] is valid for any value of $\gamma$, provided that $\gamma$ does not appear explicitly in the equations [6], and that it also holds for the linear case ($\gamma = 0$), simply removing $\gamma$ from the definition of the generalized state variables. This system will be referred to as Model 1 in the Section of Results.

In this work, together with the hydraulic nonlinearity in the damping term, a second nonlinearity is introduced, that represents a nonlinear (cubic) stiffening term in the undercarriage elastic response. The lateral translation equation is thus re–written in the form

$$\ddot{x} + (2n_0 + \gamma|\dot{x}|)\dot{x} + p_0^2(1 \pm \delta^2 x^2)x = (S/M)\ddot{\eta}$$

where the plus and the minus sign hold for a stiffening and a softening cubic nonlinearity, respectively. This last equation can be recast in terms of generalized variables as

$$\tilde{x}'' + (2\tilde{n}_0 + |\tilde{x}'|)\tilde{x}' + (1 \pm \tilde{\delta}^2\tilde{x}^2)\tilde{x} = \tilde{\eta}'' \tag{10}$$

where $\tilde{\delta} = \delta/\gamma$ provides a measure of the relative size of the nonlinear terms included in the model.

Note that, if $\gamma = 0$ and $\delta \neq 0$, it is possible to define a new set of generalized variables, replacing $\gamma$ with $\delta$ in their definition, so that the resulting system becomes

$$\tilde{x}'' + 2\tilde{n}_0\tilde{x}' + (1+\tilde{x}^2)\tilde{x} = \tilde{\eta}'' \quad (11)$$

$$\tilde{\eta}'' + 2\tilde{n}_b\tilde{\eta}' + \tilde{\omega}_s^2\eta - 2\tilde{\omega}(\tilde{\phi}' + \tilde{n}_b\tilde{\phi}) = \epsilon\tilde{x}'' \quad (12)$$

$$\tilde{\phi}'' + 2\tilde{n}_b\tilde{\phi}' + \tilde{\omega}_s^2\phi + 2\tilde{\omega}(\tilde{\eta}' + \tilde{n}_b\tilde{\eta}) = 0 \quad (13)$$

This latter system will be referred to as Model 2. It can be observed that the describing function approach [7] adopted by Tongue for successfully dealing with the nonlinear damping term is hardly applicable to the cubic nonlinearity in the elastic response of the undercarriage structure. The describing function approach is based upon the definition of an equivalent first harmonic term which reproduces the fundamental features of the nonlinearity introduced in the system. The amplitude of the additional term depends nonlinearly on the frequency of the forcing term and the amplitude of the resulting motion, so that the system is no longer truly linear. At the same time the system response frequency exactly matches that of the forcing term, as for standard linear systems. Hence the term "quasi–linearization" adopted for this procedure.

Cubic nonlinearities, on the converse, always cause a system response with content over two different frequencies, $\omega$ (the frequency of the forcing term) and $3\omega$ . This can be easily understood by considering the trigonometric equivalence $\mathrm{Cos}^3(x) = 0.75\mathrm{Cos}(x) + 0.25\mathrm{Cos}(3x)$. By retaining the fundamental frequency only, a sizable error would result inasmuch as 25% of the signal due to the nonlinear term is neglected. On the converse, the collocation method adopted in the discretization of the limit cycle during the continuation process allows for a more accurate approximation of the periodic solutions for the nonlinear model in its original formulation, so that a better understanding of the actual features of the post–critical behaviour of the system is achieved.

## 2.2 Continuation method and bifurcation analysis

A continuation algorithm [1] is a numerical technique that allows one to trace branches of solutions for a set of nonlinear algebraic equations in the form

$$\boldsymbol{f}(\boldsymbol{x}, \lambda) = \boldsymbol{0},\ \boldsymbol{x} \in \mathbb{R}^n,\ \lambda \in \mathbb{R} \quad (14)$$

as the continuation parameter $\lambda$ is smoothly varied. If the vector field $\boldsymbol{f} : \mathbb{R}^n \times \mathbb{R} \mapsto \mathbb{R}^n$ is at least Lipschitz continuous, the branch of solutions $\boldsymbol{x}(\lambda)$ is also (locally) smooth, with the exception of singular points where several branches of solutions may intersect [3].

In order to follow locally vertical branches, continuation is not performed with respect to the actual continuation parameter, $\lambda$, but by use of an auxiliary variable, the pseudo–arc–length $s$, so that the Jacobian matrix of the augmented system

$$\begin{aligned} \boldsymbol{f}(\boldsymbol{x}(s), \lambda(s)) &= \boldsymbol{0} \\ (\mathrm{d}\boldsymbol{x})^2 + (\mathrm{d}\lambda)^2 &= (\mathrm{d}s)^2 \end{aligned}$$

is not singular when the function $\boldsymbol{f}(\boldsymbol{x}, \lambda)$ is not invertible with respect to $\lambda$.

A prediction–correction method is employed, where a first approximation of the solution $\boldsymbol{x}^{(0)}$ for a perturbed value $\lambda + \delta\lambda$ is obtained from the knowledge of previous solutions (prediction step). The approximation is then refined (correction step) by a numerical technique such as Newton or Newton–chord iterative schemes until a prescribed tolerance is reached, $||\boldsymbol{f}(\boldsymbol{x}^{(k)}, \lambda + \delta\lambda)|| < \varepsilon_f$ and $||\boldsymbol{x}^{(k)} - \boldsymbol{x}^{(k-1)}|| < \varepsilon_x$. If no convergence is achieved, a new iteration is attempted reducing the continuation step $\delta\lambda$. The method requires the knowledge of at least one initial solution of Eq. (14) for $\lambda = \lambda_0$.

If $\boldsymbol{f}$ represents the vector field of a dynamic system described by the set of $n$ nonlinear ordinary differential equations (ODE) in the form

$$\dot{\boldsymbol{x}} = \boldsymbol{f}(\boldsymbol{x}, \lambda), \quad (15)$$

those points $(\boldsymbol{x}, \lambda) \in \mathbb{R}^n \times \mathbb{R}$ where $\boldsymbol{f} = 0$ are equilibria for the system and singular points where the Jacobian $\nabla\boldsymbol{f}$ becomes singular are accompanied by changes of stability of steady states along the branch, that is, bifurcations.

In the present case, Hopf bifurcations [3] are expected along the branch of equilibria where $x = \eta = \phi = 0$, inasmuch as loss of stability is induced by a pair of complex conjugate eigenvalues crossing the imaginary axis. Hopf bifurcations are accompanied by the presence of a branch of limit cycles, that is, periodic solutions $\hat{\boldsymbol{x}}(t)$ of the set of ODEs, such that $\hat{\boldsymbol{x}}(t) = \hat{\boldsymbol{x}}(t+T)$, where $T$ is the period of the solution [11]. A branch of stable periodic solutions may surround the unstable equilibrium branch (supercritical case) or a branch of unstable limit cycles circles around the stable branch of steady states (subcritical case).

Continuation of periodic solutions is dealt with by defining a two–point boundary value problem,

where a non–dimensional time $\tau = t/T$ is introduced and the limit cycle $\hat{\boldsymbol{x}}(\tau)$ satisfies the conditions

$$\hat{\boldsymbol{x}}' = T\boldsymbol{f}(\hat{\boldsymbol{x}}, \lambda) \ , \quad \hat{\boldsymbol{x}}(0) = \hat{\boldsymbol{x}}(1) \qquad (16)$$

where $\boldsymbol{x}' = \mathrm{d}\boldsymbol{x}/\mathrm{d}\tau = T\mathrm{d}\boldsymbol{x}/\mathrm{d}t = T\dot{\boldsymbol{x}}$. The periodic solution is discretized using orthogonal collocation. The limit cycle is divided into $N$ intervals, inside which the solution is represented by an expansion in terms of Lagrange polynomials of order 0 up to $m$, where $m$ is the number of Gauss collocation points per interval [2]. In this way the problem of finding a periodic solution for Eq. (15) is transformed into standard form, Eq. (14), as the resulting discretized orbit must satisfy a set of $Nm + 1$ equations ($Nm$ collocation points plus the periodicity condition) in $Nm + 1$ unknowns, where the unknowns are the $Nm$ coefficients of the piecewise Lagrange polynomial expansion of the periodic solution plus the limit cycle period. A further integral condition is needed in order to solve for the phase indeterminacy, as if $\hat{\boldsymbol{x}}(\tau)$ is a solution of Eq. (15), also $\hat{\boldsymbol{x}}(\tau + \sigma)$ satisfies the same equation. Details on this last issue can be found in [2].

Stability of limit cycles is investigated using an approximation of the linear part $\boldsymbol{M}$ of the Poincaré map [2, 3], which is obtained as a by–product of the numerical technique for continuation of periodic solutions. The eigenvalues of $\boldsymbol{M}$, namely the Floquet multipliers, provide the desired information on cycle stability. Floquet multipliers can be either very large or very small. In both cases their determination based on an approximation of $\boldsymbol{M}$ becomes critical and sudden variations may lead to sizable errors in the determination of the bifurcation point along the branch of limit cycles. Nonetheless, they are used to determine the presence of secondary periodic bifurcations (branch point and bifurcations to torii), and direct numerical simulation will be used in those cases when the approximation is considered not reliable.

Several implementations of the numerical continuation algorithm are available, with the capability of detecting bifurcations, performing branch switching when pitchfork bifurcations are encountered, or finding branches of periodic solutions bifurcating from Hopf points. Among many others, one of the most widely used was developed by Doedel and his co–workers [12], which runs on Unix and Linux platforms. In this paper, branches of equilibria and periodic solutions were traced by means of the freely available continuation software MatCont [13], that exploits similar numerical techniques and runs in Matlab$^{\mathrm{TM}}$ environment

# 3 Results

The stability boundaries that mark the onset of ground resonance oscillations are independent of the type of nonlinearity introduced in the model. As a first application of continuation methods, the determination of these boundaries for the linear constant coefficient case as a function of system parameters was performed. In order to trace these plots, Eqs. (7)–(9) (without the nonlinear term $|\tilde{x}'|$ in the damping coefficient) were recast into matrix form and transformed into the Laplace variable domain, that is

$$(\boldsymbol{M}s^2 + \boldsymbol{C}s + \boldsymbol{K})\bar{\boldsymbol{y}}(s) = 0$$

where $\boldsymbol{y} = (\tilde{x}, \tilde{\eta}, \tilde{\phi})^T$. The eigenvalues of the system are determined from the equation

$$\det(\boldsymbol{M}\lambda^2 + \boldsymbol{C}\lambda + \boldsymbol{K}) = 0$$

and the equilibrium condition $\boldsymbol{y}_e = (0, 0, 0)^T$ becomes unstable as soon as the real part of one of the 3 pairs of conjugate eigenvalues that characterize the eigenstructure of the system becomes positive.

The eigenvalues depend on system parameters, namely $\epsilon$, $\nu_0$, $\tilde{n}_0$, $\tilde{n}_b$, and $\tilde{\omega}$. Two of the parameters, $\tilde{\epsilon}$ and $\tilde{\nu}_0$, are determined by the inertial properties of rotor blades, and they will be assumed as prescribed. On the converse, rotor spin rate $\tilde{\omega}$ will vary during rotor engagement and disengagement operations, and it must be left free to vary during the analysis. At this point it is possible to investigate rotor–fuselage stability as a function of $\tilde{\omega}$ and fuselage and rotor blade damping parameters, $\tilde{n}_0$ and $\tilde{n}_b$. The equation for the stability boundary can be written in the form

$$f(\tilde{n}_0, \tilde{n}_b, \tilde{\omega}) = \max_k[\lambda_k] = 0 \qquad (17)$$

which is solved for different, prescribed values of $\tilde{n}_0$. The resulting plots in the $\tilde{n}_b$–$\tilde{\omega}$ plane, reported in Fig. 2, were obtained by means of the continuation method. For every value of $\tilde{n}_0$, the point $(\tilde{n}_b, \tilde{\omega}) = (0, 0)$ satisfies Eq. (17). This can be used as the starting point for the continuation, where $\tilde{\omega}$ is the continuation parameter and $\tilde{n}_b$ is determined by the continuation software as $\tilde{\omega}$ is varied. The resulting approach is considerably more efficient than the numerical procedure outlined in [6] for obtaining the same plot.

The plots in Fig. 2 show that for $\tilde{n}_0 > \tilde{n}_{0,cr} \approx 0.72$, the stability boundary in the $\tilde{n}_b$–$\tilde{\omega}$ plane is a continuous line featuring a maximum $\tilde{n}_{b,cr}$ with

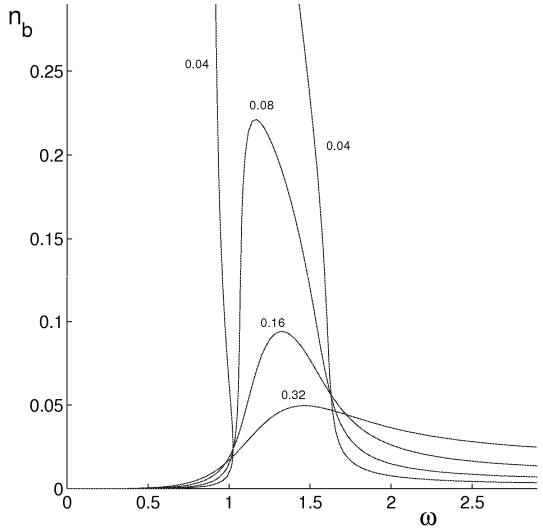


Figure 2: Stability boundaries for the linear system as a function of $\tilde{n}_b$ and $\tilde{\omega}$ ($\epsilon = 0.04$, $\nu_0 = 0.25$, $\tilde{n}_0$ indicated on the curves).

respect to the blade damping parameter, $\tilde{n}_b$. This means that, if $\tilde{n}_b$ is higher than this critical value, no ground resonance instability occurs for any value of rotor spin rate. On the converse, as already described in [6], if either $\tilde{n}_0 < \tilde{n}_{0,cr}$ or $\tilde{n}_0 > \tilde{n}_{0,cr}$ and $\tilde{n}_b < \tilde{n}_{b,cr}$, there exist two critical values, $\tilde{\omega}_1$ and $\tilde{\omega}_2$, where Hopf bifurcations are encountered. These values bound an interval on the $\tilde{\omega}$ axis, where the equilibrium is unstable and ground resonance oscillations are expected to take over.

Three configuration for the post–critical behaviour are possible, which are reported qualitatively in Fig. 3.a–c, where thick lines indicate the amplitude of the oscillations, while thin lines are associated to branches of equilibria. Continuous lines are used for stable steady states, while dashed ones indicate unstable solutions. When both Hopf bifurcations are supercritical (Case a) bounded oscillations are present for $\tilde{\omega}_1 < \tilde{\omega} < \tilde{\omega}_2$, which disappears as soon as the value of $\tilde{\omega}$ leaves the unstable interval. Provided that the amplitude of the oscillations at steady–state between the two critical values remains limited and/or the critical interval is crossed in a sufficiently short time so that the oscillations cannot fully develop, the instability may not lead to a catastrophic behaviour.

A more serious instability is present if the configuration depicted in Fig. 3.b is dealt with. In this case (Case b), the Hopf bifurcation in $\tilde{\omega}_2$ is subcritical. This means that there exists a fold on the branch of limit cycles, and the portion of the stable equilibrium branch for $\tilde{\omega}_2 < \tilde{\omega} < \tilde{\omega}_F$ is surrounded by unstable periodic solutions. In such a

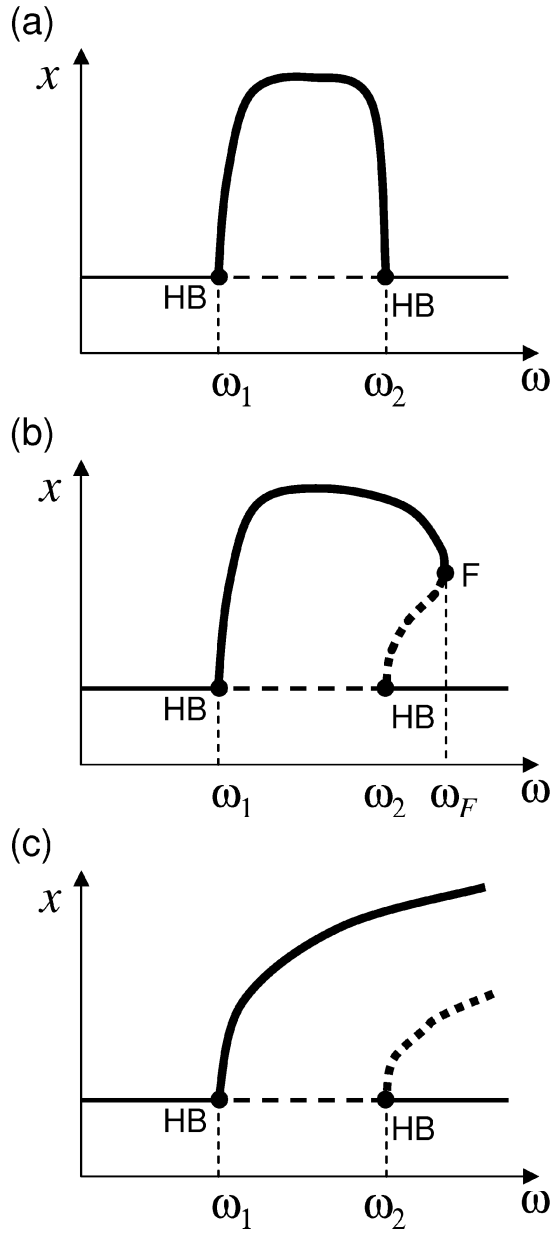


Figure 3: Types of post–critical behaviour.

case, a jump is present so that the ground resonance oscillations are likely to fully develop while $\tilde{\omega}$ increases beyond $\tilde{\omega}_1$, suddenly disappearing as soon as $\tilde{\omega} > \tilde{\omega}_F$. In this scenario the amplitude reached by either blade or fuselage oscillations is likely to exceed structural limits.

An even more catastrophic situation is encountered for those values of $\tilde{n}_b$ and $\tilde{n}_0$ that lead to a configuration of limit cycles like that depicted in Fig. 3.c. In this latter case (Case c) no fold is present on the stable branch of limit cycles, with oscillations of increasing amplitude as $\tilde{\omega}$ grows. Moreover, the whole stable branch of equilibria for $\tilde{\omega} > \tilde{\omega}_2$ is surrounded by unstable limit cycles, which means that its stability is only local. During

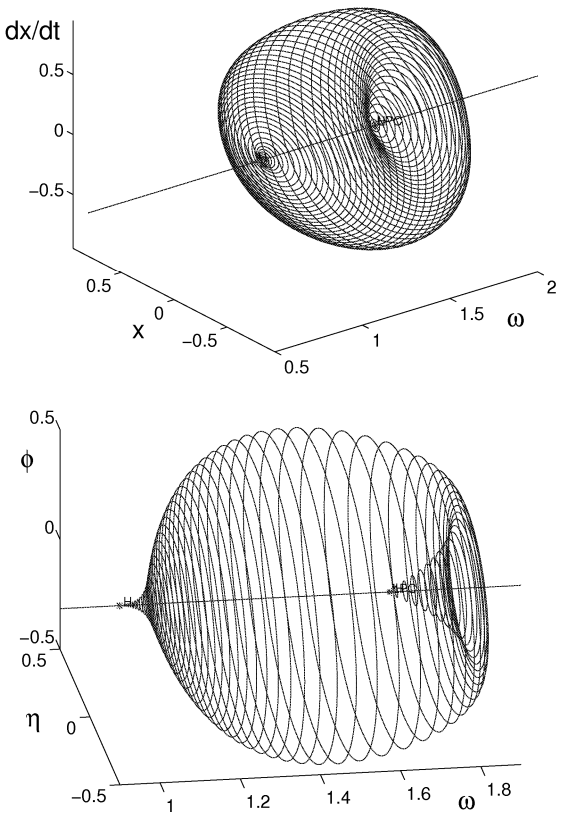


Figure 4: Model 1: Limit cycles as a function of $\omega$ ($\epsilon = 0.04$, $\nu_0 = 0.25$, $n_0 = 0.02$, $n_b = 0.04$).

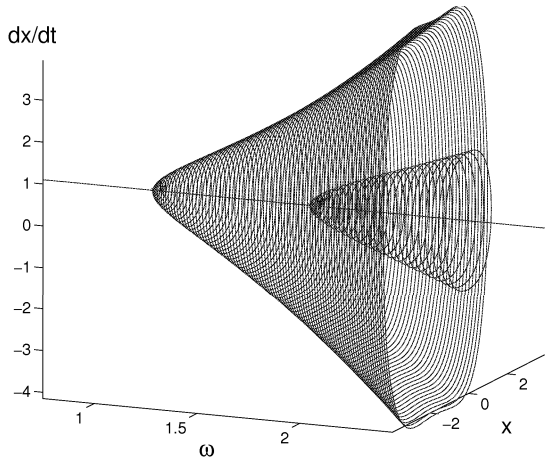


Figure 5: Model 2: Limit cycles as a function of $\omega$ ($\epsilon = 0.04$, $\nu_0 = 0.25$, $n_0 = 0.02$, $n_b = 0.04$).

rotor spin–up, the oscillations induced by the instability for $\tilde{\omega} > \tilde{\omega}_1$ will not disappear when $\tilde{\omega}$ grows beyond $\tilde{\omega}_2$, in spite of the stability of the underlying equilibrium. This behaviour, confirmed by direct numerical simulation not reported in the figures, is due to the fact that the oscillations grow in amplitude as $\tilde{\omega}$ is increased, moving along the stable periodic solution branch that surrounds the unstable one. This prevents the system from achieving a new stable equilibrium when $\tilde{\omega} > \tilde{\omega}_2$.

A Case b configuration is reported in Figs. 4.a and b, where a continuation with respect to $\tilde{\omega}$ is performed for the hydraulic nonlinearity (Model 1). The shape of the limit cycles clearly presents a fold which would induce an histeretic behaviour, as already outlined by Tongue [6].

When a cubic nonlinearity in the stiffness term is considered (Model 2), a Case c configuration is encountered for the same values of the damping parameters (Fig. 5). This fact clearly shows that the stiffening term has dramatic consequences on the configuration of the limit cycles. Only when higher values of the damping parameters are considered, the structure of the limit cycles become less catastrophic. This clearly indicates that the presence of stiffening terms can be detrimental, if not properly taken into account in the design phase. Note also that the shape of the limit cycles on the stale branch in the $\tilde{x}$–$\tilde{x}'$ plane is quite different from the elliptical one that would have been obtained from the application of the describing function approximation.

# 4 Conclusions

The analysis of postcritical behaviour of a simple helicopter model aimed at representing basic features of the ground resonance phenomenon was dealt with by means of continuation software and bifurcation analysis. The analysis demonstrates that, in presence of cubic stiffening terms in the elastic response of the undecarriage structure, a catastrophic scenario is encountered, where the presence of a subcritical Hopf bifurcation prevents the oscillations from stopping even if the rotor is accelerated beyond the critical threshold where stable equilibria for the rotor–fuselage system do exist. As an advantage with respect to previous approaches, the proposed method allows for a more accurate determination of the features of the oscillations (shape and amplitude) sparked by the instability.

Future work will be aimed at extending the study to more complex models where hydraulic and cubic stiffening terms are simultaneously present. Also, a detailed analysis of an individual blade model, where a full order dynamical system featuring lag dynamics of every single blade will be considered, rather than the reduced order one used in the present work. In this more complete model, lag stops will also be modeled as sudden increases of

blade lag spring stiffness, a feature that is expected to introduce further variations on the topology of the system solutions after the onset of ground resonance.

## References


[1] Doedel E J, Keller H B, and Kernevez J P. Numerical Analysis and Control of Bifurcation Problems. Part I: Bifurcations in Finite Dimension, *Int. J. Bif. & Chaos* 1991, **1** (3), pp. 493–520.

[2] Doedel E J, Keller H B, and Kernevez J P. Numerical Analysis and Control of Bifurcation Problems. Part II: Bifurcations in Infinite Dimension, *Int. J. Bif. & Chaos* 1991, **1** (4), pp. 745-772.

[3] Guckenheimer J, and Holmes P. *Nonlinear oscillations, dynamical systems and bifurcations of vector fields*, Springer, New York, 1983.

[4] Mil M L, Nekrasov A V, Braveman A S, Grodko L N, and Leikand M. Helicopters - Calculation and Design. Vol. 2 - Vibrations and Dynamic Stability. NASA TT F-519, May 1968.

[5] Coleman R P, and Feingold, A M. Theory of Self–excited Mechanical Oscillations of Helicopter Rotors with Hinged Blades. NACA Report 1351, Feb. 1957.

[6] Tongue B H. Limit Cycle Oscillations of a Nonlinear Rotorcraft Model, *AIAA J.* 1984, **22** (7), pp. 967-974.

[7] Voronov A A. *Basic Principles of Automatic Control Theory Special Linear and Nonlinear Systems*, Mir Publishers, Moscow, 1985, Chap. 4.

[8] Goman M G, Zagainov G I, and Khramtsovsky A V. Application of Bifurcation Methods to Nonlinear Flight Dynamics Problems. *Prog. Aerosp. Sci.* 1997, **33** (9), pp. 539-586.

[9] Afolabi D. The cusp catastrophe and the stability problem of helicopter ground resonance. *Proc. Royal Soc. Math. & Ph. Sci.* 1993, **441** (1912), pp. 399-406.

[10] Sibilski K. Prediction of Helicopter Critical Flight Regimen by Continuation and Bifurcation Methods. AIAA paper 2006–6633, Atmospheric Flight Mechanics Conference, Keystone (CO), Aug. 2006.

[11] Hopf E. Abzweigung einer periodischen Lösung von einer stationären Lösung eines differential-systems. *Berichte über die Verhandlungen der Sächsischen Akademie der Wissenschaften zu Leipzig* 1942, **94**, pp. 1–22.

[12] Doedel E J, Fairgrieve T F, Champneys A R, Sandstede B, Kuznetsov Y A, and Wang X. Auto97: Continuation and Bifurcation Software for Ordinary Differential Equations (With Homcont). Technical report, Concordia University, Montreal (Canada), 1998.

[13] Dhooge A, Govaerts W, Kuznetsov Y A, Mestrom W, Riet A M, and Sautois B. CL MATCONT: A continuation toolbox in Matlab. `http://www.matcont.ugent.be/`, last update: January 22, 2007, documentation: December 2006.